

A SIMPLE AND EFFECTIVE METHOD FOR ENHANCING ITERATION CONVERGENCE OF INCOMPRESSIBLE FLUID FLOW AND HEAT TRANSFER SIMULATIONS: LAGRANGE INTERPOLATION FOR INITIAL FIELD

Z. G. Wu, J. Z. Zhang, J. J. Zhou, and W. Q. Tao

State Key Laboratory of Multiphase Flow and Heat Transfer, School of Energy and Power Engineering, Xi'an Jiaotong University, Xi'an, Shaanxi, People's Republic of China

An approach is presented for designing initial fields for a series of computations of heat transfer and fluid flow problems. Through polynomial interpolation with existing converged solutions, better initial fields are obtained for the solutions of the next case. This procedure is repeated until all the cases are numerically simulated. This method is called the interpolative initial field method. By using this method the total iteration times can be substantially reduced. In addition, the more cases are used in the interpolation, the more efficient the interpolative initial field will be.

INTRODUCTION

How to enhance iteration convergence rate in numerical simulation of fluid flow and heat transfer problems is always a research interest of the computational fluid dynamics and heat transfer community. Researchers focus mostly on either improving numerical algorithms [1–10] or using efficient matrix solution methods [10–19]. The development of the SIMPLE family of algorithms is a typical example of the first category, while adoption of TDMA [11, 12, 20], PDMA [15, 21], and SIP [17] to the Krylov subspace method [22] represent using efficient matrix solution methods. The common feature of the two categories is that the emphasis is concentrated on a single solution process.

However, for many practical problems, a group of more or less related cases is to be solved to reveal the relationship between dependent variables and independent variables. For example, in the laminar fluid flow over a rectangular backward step problem, the distance between the position of the reattachment point and the step, L_R , increases gradually with Reynolds number Re [23]. In natural-convection flow in a square cavity, the Nusselt number Nu increases with Rayleigh number

Received 4 September 2006; accepted 21 October 2006.

This work was supported by the National Natural Science Foundation of China (No. 50476046) and the State Key Program for Basic Research of China (No. 2007CB206902).

Address correspondence to W. Q. Tao, State Key Laboratory of Multiphase Flow and Heat Transfer, School of Energy and Power Engineering, Xi'an Jiaotong University, 28 Xian Ning Road, Xi'an, Shaanxi 710049, People's Republic of China. E-mail: wqtao@mail.xjtu.edu.cn

NOMENCLATURE

a	fluid thermal diffusivity	u, v	velocity component in x and y directions
A	surface area	u^*, v^*	velocity correction
D	diameter	U, V	nondimensional velocity
flow _{ch}	characteristic (reference) flow rate	U_{lid}	driven lid velocity
g	gravitational acceleration	x, y	coordinates
H_1, H_2	height defined in Figure 7	X, Y	dimensionless coordinates
l	length	α	underrelaxation factor
L	length of square cavity	β	coefficient of thermal expansion
L_1, L_R, L_2	length defined in Figure 5	δ	gap width
L_{in}, L_x	length defined in Figure 6	ΔT	temperature difference
M_{initial}	initial fields	μ	fluid dynamic viscosity
M_{result}	converged fields	ν	fluid kinetic viscosity
Pr	Prandtl number	ρ	density
q_m	mass flow rate	ω	angular velocity
Q	air-side heat transfer		
r	radius		
R	radius of tube wall; mass flow rate imbalance of control volume	Subscripts	
Ra	Rayleigh number	in	inlet; inner
Re	Reynolds number	max	maximum
RS _{cv}	relative mass flow rate imbalance of control volume	mean	averaged
		out	outlet
		total	all

Ra [24]. If the purpose of numerical simulations is to find the relationship between L_R and Re for the first case or between Nu and Ra for the second case, then a series of computations must be performed. The final computational efficiency will depend on how we obtain the series of solutions efficiently. To the authors' knowledge, little attention has been paid to this issue in the open literature.

It is well known that for nonlinear problems, the initial fields have great effects on the iterative numerical solution process. While "good" initial fields can shorten the iterative time, bad initial fields may even lead to the divergence of iteration [20]. Therefore, how to design initial fields is a very important issue in a series of numerical computations. In the past years, a common approach has been using the previous solutions as the initial fields for a successive computation [24].

In the numerical design of a new type of fin-and-tube heat exchanger, the present authors conducted several series of numerical computations to reveal the relationships between Nu and Re and between f and Re. In this practice, we developed a rather efficient numerical method for a series of computations. It is called the interpolative initial field method. In the following, the developed numerical method will first be introduced, followed by the presentation of seven application examples and comparisons with conventional step-by-step methods. Finally, some conclusions will be summarized.

NUMERICAL METHODS

Basic Idea of the Interpolative Initial Field Method

Assume that a series of numerical simulations are going to be conducted for steady-state, incompressible, and laminar fluid flow and heat transfer in a certain

geometric configuration with a fixed grid system. The basic independent variable, say Reynolds number, is subject to change within a wide range of variation. Apart from the upper and lower limitations of the independent variable, several intermittent points are required. For the computations of the intermittent cases, the initial fields can be obtained from existing results by interpolation. Here the computation order plays an important role. When a series of computations is to be conducted, the first/beginning case has to be completed with arbitrary assumed initial fields, followed by the second/end case of the series with the converged result fields of the first case as the initial fields. Based on the results of these two cases, we adopted the interpolation method to design the initial fields of the third case, located at the center point of two end cases. Once the third case is solved, its results and the previous two results are employed for the next case. Using dichotomy for selecting the new point, more cases can be solved, and more converged results are adopted for interpolation.

The basic idea of the interpolative initial field method can be summarized as follows.

1. Conduct the simulation for the case with the lower limitation of the independent variable with initial fields determined by a conventional method, say zero initial fields.
2. Conduct the simulation for the case with the higher limitation of the independent variable, with the solutions of the lower limitation of the independent variable as the initial fields.
3. Conduct the simulation for the middle point between the upper and lower limitations of the independent variable. This may be a middle point in the logarithmic scale, depending on the individual problem. The term “middle” is a qualitative description, not necessarily the exact middle between the upper and lower limitations, depending on the given conditions. For this case the Lagrangian polynomial interpolation method is used to get the initial fields from the two existing solutions.
4. Perform more simulations within the variation range of the independent variables with the interpolative initial fields. All the existing solutions should be used for the interpolation of the initial fields for a new case. The more the existing solutions are used in the interpolation, the more efficient the interpolative initial field method will be.

Expression for Field Interpolation

The Lagrange interpolation expression can be written as [25]

$$L_n(x) = \sum_{i=1}^n \left(\prod_{\substack{j=1 \\ j \neq i}}^n \frac{x - x_j}{x_i - x_j} \right) f(x_i) \quad (1)$$

where n is the case number for which the solutions are known. It should be noted that in Eq. (1), the variable x represents the independent parameter and $f(x_i)$ is the function of the parameter to be interpolated. For example, when natural convection in an enclosure is simulated, and we have obtained the solutions (velocity, temperature distributions) for $Ra = 1,000$ and $100,000$, the initial fields for velocity and

temperature distributions for $Ra = 10,000$ are to be interpolated. Then for this case Ra is the independent variable x , and velocity and temperature distributions are the function $f(x_i)$. The truncation error of the Lagrange interpolation polynomial is expressed as

$$R_n(x) = f(x) - L_n(x) = \frac{1}{(n+1)!} f^{(n+1)}(\xi) \pi_{n+1}(x) \quad (2)$$

It can be seen that the more cases are used in the interpolation, the smaller the truncation error of the initial fields will be.

The converged results, U , V , P , and T fields corresponding with the characteristic number, say Re , can replace $f(x_i)$ and x_i in Eq. (1), respectively. Through interpolation with known converged fields, the new fields of variables (U , V , P , and T) can be obtained.

When the logarithmic scale is used to express the numerical results, such as Nu versus Re , the position where the initial field is to be interpolated is better determined by the logarithmic scale. Taking the Lagrange interpolation expression as an example, the following expressions can be obtained:

$$Re = \frac{ul}{\nu} \quad (3)$$

$$f(u_i) = f(Re_i) \quad (4)$$

$$L_n[\log(u)] = \sum_{i=1}^n \left[\prod_{\substack{j=1 \\ j \neq i}}^n \frac{\log(u) - \log(u_j)}{\log(u_i) - \log(u_j)} \right] f(u_i) \quad (5)$$

$$\begin{aligned} L'_n[\log(Re)] &= \sum_{i=1}^n \left[\prod_{\substack{j=1 \\ j \neq i}}^n \frac{\log(Re) - \log(Re_j)}{Re_i - Re_j} \right] f(Re_i) \\ &= \sum_{i=1}^n \left[\prod_{\substack{j=1 \\ j \neq i}}^n \frac{\log(ul/\nu) - \log(u_j l/\nu)}{\log(u_i l/\nu) - \log(u_j l/\nu)} \right] f(Re_i) \\ &= \sum_{i=1}^n \left[\prod_{\substack{j=1 \\ j \neq i}}^n \frac{\log(u) - \log(u_j)}{\log(u_i) - \log(u_j)} \right] f(u_i) \\ &= L_n[\log(u)] \end{aligned} \quad (6)$$

In order to compare the computation time, the step-by-step initial fields method is also used, for which the initial field setup can be expressed as

$$M_{\text{initial}}^{i+1}(u) = M_{\text{result}}^i(u) \quad (7)$$

where the superscript stands for the case number. Such a practice has been widely used in the literature [25], and compared with the arbitrary field assumptions for every case, this step-by-step method, i.e., a previous converged result, used as the initial field of the next computation, can also enhance the convergence rate.

Numerical Comparison Conditions

For a meaningful comparison between step-by-step initial fields and the Lagrange interpolation initial fields method, the same simulation code should be used. And except for the initial fields, the other numerical treatment should be the same, too. In the following comparison, the numerical treatments for computation are introduced as follows.

For the coupling between velocity (U , V) and pressure (P), the SIMPLEX [3] algorithm is employed. Using an absolutely stable and simple scheme, the power-law scheme [5], can keep the stability of the solution procedure. The algebraic equations are solved by the alternating-direction implicit method (ADI) incorporating the block-correction technique [1]. For all the cases studied, the same value is adopted for the underrelaxation factor α . The convergence criterion is written as follows:

$$Rs_{cv} = \text{MAX}_{cv} \left[\frac{(\rho u^* A)_w - (\rho u^* A)_e + (\rho v^* A)_s - (\rho v^* A)_n}{\text{flow}_{ch}} \right] \leq \varepsilon \quad (8)$$

where the nondimensional Rs_{cv} is the maximum mass residue of all control volumes, which represents the mass conversion degree of each control value. The value ε is different for different problems, and is uniform for all cases in the same problem.

These two initial field setup methods are applied to six two-dimensional problems and one three-dimensional problem of fluid flow and heat transfer. They are (1) lid-driven cavity flow in a square cavity, (2) lid-driven cavity flow in a polar cavity, (3) laminar fluid flow over a rectangular backward-facing step, (4) laminar fluid flow over an annular backward step, (5) natural convection in a square cavity, (6) natural convection in an annulus enclosure, and (7) three-dimensional fluid flow and heat transfer in a slit fin surface. These seven problems are all based on the following assumptions: laminar, incompressible, steady-state, and constant fluid property. Because of space limitations, the governing equations of each problem are omitted; they can be found in other documentation [5, 20].

The iteration number for obtaining a converged solution, and the total iteration number, are compared.

NUMERICAL EXPERIMENTS

To simplify the description, the three methods and the meanings of other special words are defined as follows.

Method A: computation with zero initial fields.

Method B: computation with previous converged fields as initial fields, or step-by-step initial fields. For a series of computations, the first point is computed by Method A, then the neighboring second point is computed with the

converged solution of the first point as the initial field. For the rest of the points, this procedure is repeated until the last point is reached.

Method C: computation with interpolative initial fields. For a series of computations the first and second points are the beginning and end points. In the computation of the second points, the converged solutions of the first point are used as the initial fields. Then the points between the two end points are computed with interpolative initial fields.

Order: the computation order with Method C.

Number: iteration number.

Points: the total number of cases computed in a series of computations.

Total: the total iteration number for all cases.

Problem 1: Lid-Driven Cavity Flow in a Square Cavity

This problem has been studied by Ghie et al. [7]. The computational configuration and the results of stream function are shown in Figure 1, where x and y are nondimensional coordinates, normalized by the cavity height. A uniform grid of 102×102 is employed. Calculations are conducted for from $Re = 10$ to 1,000. The Reynolds number is defined by

$$Re = \frac{U_{lid}L}{\nu} \quad (9)$$

The iteration numbers are listed in Tables 1 and 2 (16 points for Methods A and C, respectively), Tables 3, 5, and 7 (5, 9, and 16 points for Method B, respectively). In Tables 4, 6, and 8, the ratios of iteration number of the three kinds of methods are presented. It can be seen that for 5, 9, and 16 points, the ratio of saving of iteration numbers for Method B to Method A are 15.63%, 21.06%, and 33.55%, respectively; for Method C to Method A, 33.78%, 45.30%, and 62.38%, respectively; and for Method C to Method B, 21.5%, 30.70%, and 43.39%, respectively. The saving in iteration number is appreciable.

In Figures 2 and 3, parts of initial fields and final converged fields from Methods A and C are compared. For $Re = 100$, its interpolation order is third-order (i.e., two existing solutions are used). Though its tendency is approximately similar, the value is far away from the converged fields. And from Tables 2 and 7, it can be seen that the iteration number with Method C is 1,442, larger than with Method B, which is 976. For $Re = 50$, the interpolation order is 12th-order (i.e., 11 existing solutions are used). It can be seen that parts of the initial fields are nearly the same as the converged fields. Thus, the iteration number with Method C is 72, far less than that with Method B, 1,201 (see Tables 2 and 7). In Table 8 the savings in total iteration numbers are summarized for the 16-points situation. Method C can save 62.4% over Method A and 43.4% over Method B. The interpolated initial fields are very effective.

In Table 9, the iteration numbers for different points are listed. For the beginning situation (5 points), the required iteration numbers are listed in the first column. For the second situation (9 points), the extra iteration numbers required to obtain the converged solution are expressed by + XXXX. As can be seen from the table,

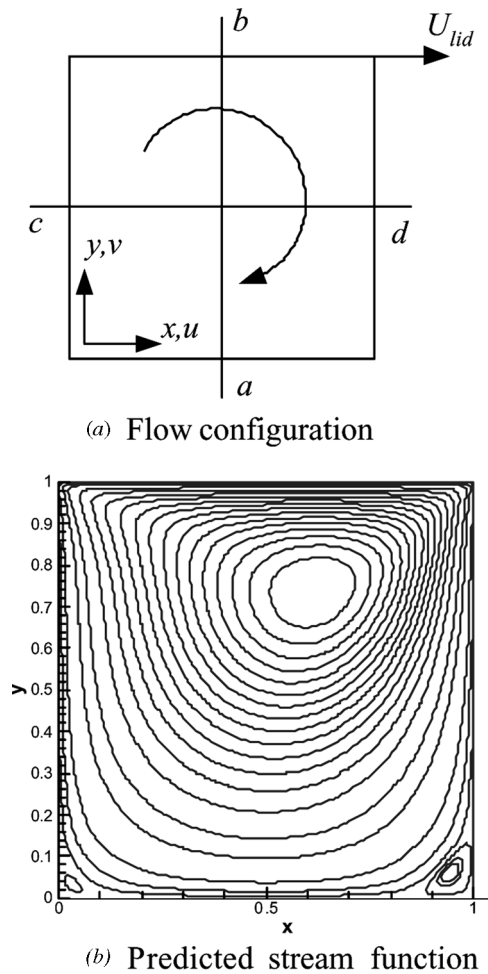


Figure 1. Lid-driven cavity flow in a square cavity ($Re = 100$): (a) flow configuration; (b) predicted stream function.

Method C offers a great advantage in saving of total iteration number. And the more points there are, the more efficient the interpolative initial fields method is. For the situation of 16 points, the required iteration numbers for Method C are only $1/3.39$ of that of Method B.

Table 1. Computation with Method A for 16 points (first example)

Re	10	17.8	30	31.6	50	56.2	80	100
Number	2,226	2,569	1,314	2,434	2,113	2,222	2,638	3,252
Re	120	178	300	316	500	562	800	1,000
Number	4,248	3,241	3,116	3,103	2,812	3,234	3,042	3,680

Table 2. Computation with Method C for 16 points (first example)

Re	10	17.8	30	31.6	50	56.2	80	100
Order	<i>1</i>	<i>6</i>	<i>10</i>	<i>4</i>	<i>12</i>	<i>8</i>	<i>14</i>	<i>3</i>
Number	2,226	1,151	55	1,014	72	1,233	88	1,442
Re	120	178	300	316	500	562	800	1,000
Order	<i>16</i>	<i>9</i>	<i>11</i>	<i>5</i>	<i>13</i>	<i>7</i>	<i>15</i>	<i>2</i>
Number	113	1,014	191	1,707	445	1,072	1314	3,342

Table 3. Computation with Method B for 5 points (first example)

Re	10	31.6	100	316	1,000
Number	2,226	979	3,055	2,207	3,931

Table 4. Comparison with total iteration number for 5 points in Table 3 (first example)

	Method A	Method B	Method C
Total	14,695	12,398	9,731
		$(14,695 - 12,398)/14,695 = 15.63\%$	$(14,695 - 9,731)/14,695 = 33.78\%$ $(12,398 - 9,731)/12,398 = 21.5\%$

Table 5. Computation with Method B for 9 points (1–9 in Table 2) (first example)

Re	10	17.8	31.6	56.2	100	178	316	562	1,000
Number	2,226	1,976	1,458	1,737	2,496	2,203	2,274	3,291	2,832

Table 6. Comparison with total iteration number for 9 points in Table 5 (first example)

	Method A	Method B	Method C
Total	25,961	20,493	14,201
		$(25,961 - 20,493)/25,961 = 21.06\%$	$(25,961 - 14,201)/25,961 = 45.30\%$ $(20,493 - 14,201)/20,493 = 30.70\%$

Table 7. Computation with Method B for all 16 points in Table 2 (first example)

Re	10	17.8	30	31.6	50	56.2	80	100
Number	2,226	1,976	834	1,195	1,201	1,049	1,448	976
Re	120	178	300	316	500	562	800	1,000
Number	858	3,241	2,061	799	2,812	3,234	3,042	3,114

Table 8. Comparison of total iteration number for all 16 points in Table 7 (first example)

	Method A	Method B	Method C
Total	45,244	30,066	17,021
		$(45,244 - 30,066)/45,244 = 33.55\%$	$(45,244 - 17,021)/45,244 = 62.38\%$ $(30,066 - 17,021)/30,066 = 43.39\%$

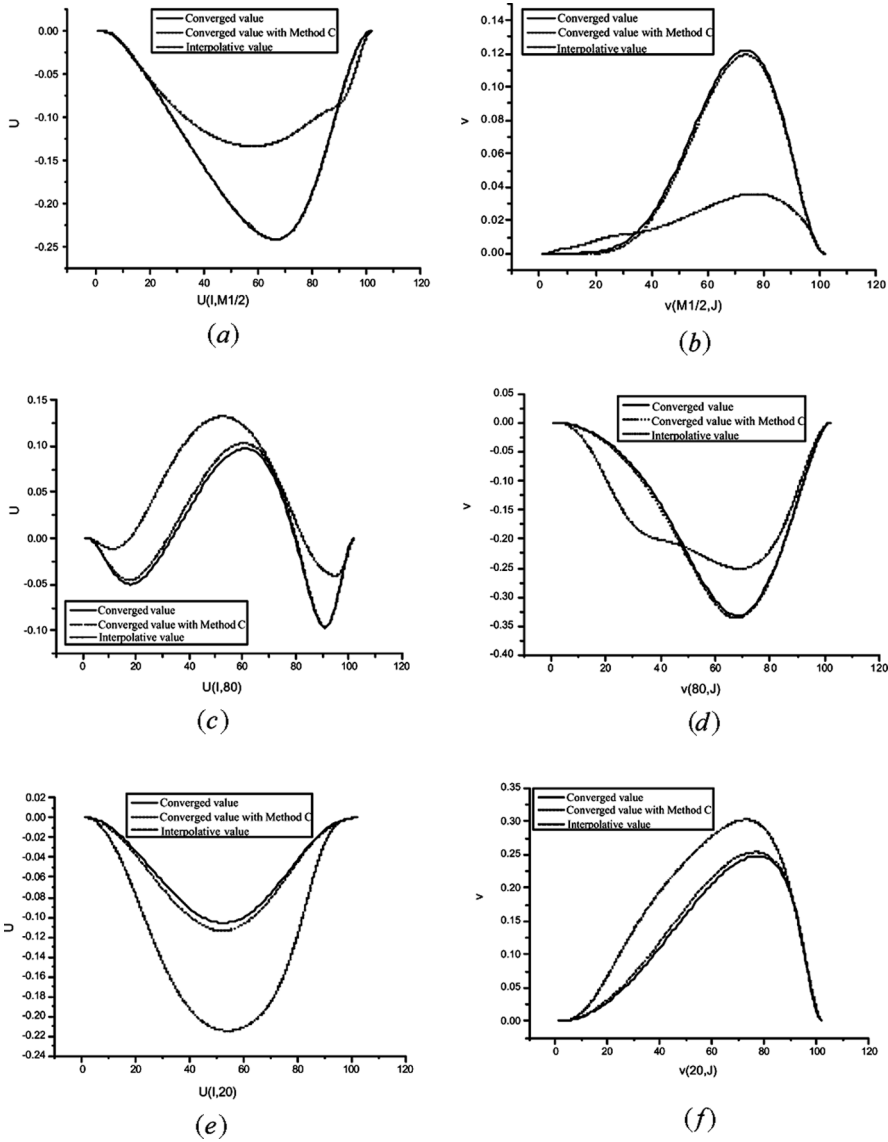


Figure 2. Parts of initial fields and converged fields with Method A and Method C for $Re = 100$.

Problem 2: Lid-Driven Cavity Flow in a Polar Cavity

The configuration and its converged stream function are shown in Figure 4 ($\theta = 1$ radian, $\delta/R_{in} = 1$). This problem was studied by Fuchs and Tillmark using both experimental and numerical methods [26]. The Reynolds number is defined as

$$Re = \frac{R_{in} \cdot \omega \cdot \delta}{\nu} \tag{10}$$

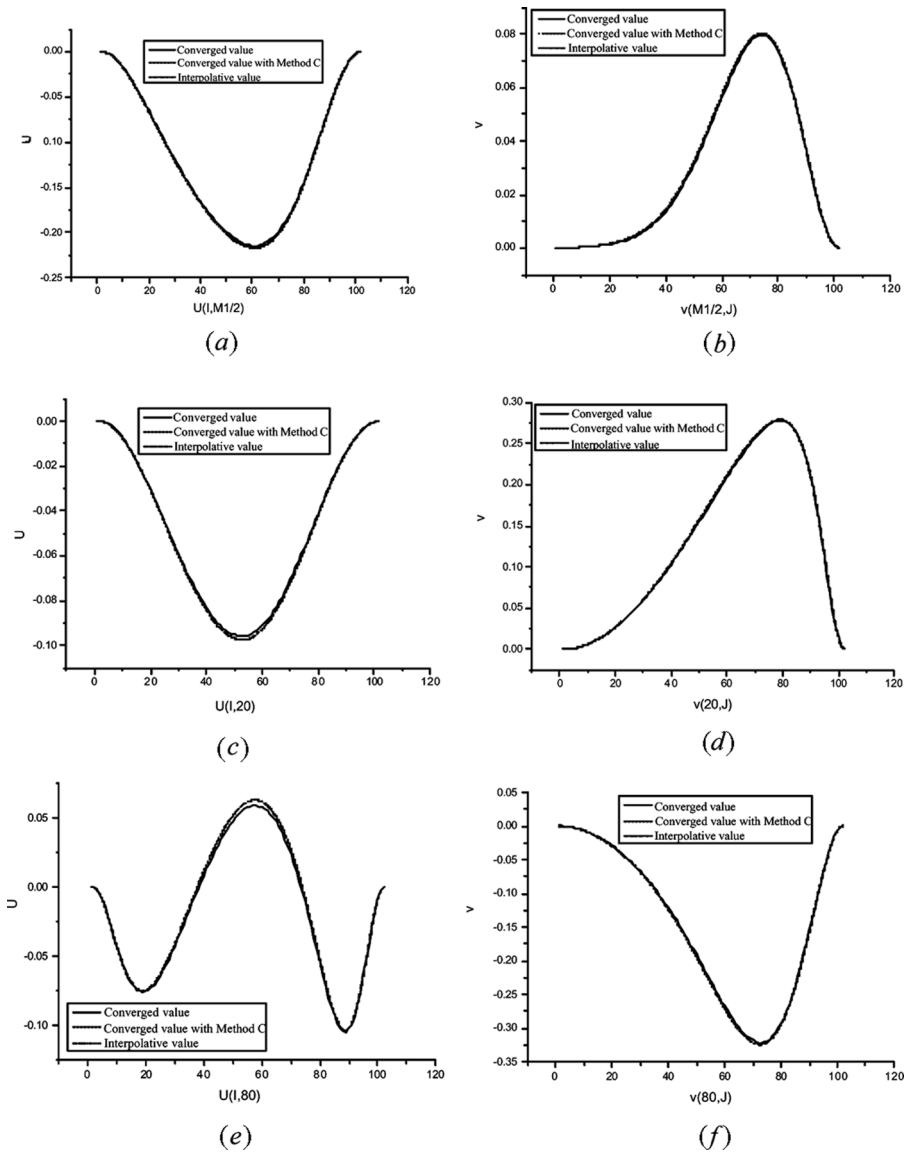


Figure 3. Parts of initial fields and converged fields with Method A and Method C for $Re = 50$.

Table 9. Iteration numbers for different points (first example)

Number of points	5	9 (= 5 + 4)	16 (= 9 + 7)
Method A	14,695	+ 11,266	+ 19,283
Method B	12,398	+ 8,095	+ 9,573
Method C	9,731	+ 4,470	+ 2,820

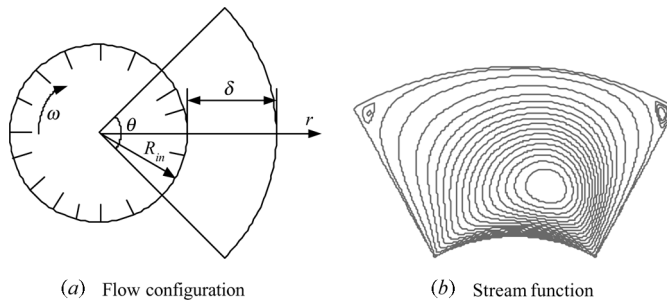


Figure 4. Lid-driven cavity flow in a polar cavity (Re = 100).

Our computations are conducted on a grid system of 102×102 , with Reynolds number ranging from 10 to 1,000.

The same comparison process can be made as for the first case. For simplicity of presentation, only the saving in the total iteration numbers for 5, 9, and 16 points are presented in Tables 10, 11, and 12. For the three situations, the related Reynolds numbers are listed after each table. As can be expected from the tables, the intermittent points are determined in the logarithmic scale for the situation with 5 and 9 points. For the other situation the extra points are added randomly. From Tables 10, 11, and 12, it can be observed that the saving of iteration numbers using Method C over Method A for the three situations range from 47.9% to 72%. The saving of iteration number is appreciable.

Problem 3: Laminar Fluid Flow over a Rectangular Backward Step

The problem configuration and its converged stream function are shown schematically in Figure 5. The geometric parameters are taken from Kondoh et al. [23]: $H_2/H_1 = 2$, $L_1/H_1 = 5$, $L_2/H_1 = 30$. The inlet velocity distribution is fully developed:

$$X = 0, \quad 1 < Y < \frac{H_1 + H_2}{2} : \quad U = 1.5 \left\{ 1 - \left[\frac{Y - 0.5(H_2/H_1) - 1}{0.5(H_2/H_1)} \right]^2 \right\}, \quad V = 0 \tag{11}$$

Table 10. Comparison with total iteration number for 5 points (second example)

	Method A	Method B	Method C
Total	8,788	4,902 (8,788 - 4,902)/8,650 = 44.93%	4,644 (8,788 - 4,644)/8,650 = 47.91% (4,902 - 4,644)/4,902 = 5.26%
Re	10	31.6	100
			316
			1,000

Table 11. Comparison with total iteration number for 9 points (second example)

	Method A		Method B			Method C			
Total	14,176		6,642 (14,176 – 6,642)/14,176 = 53.15%			5,726 (14,176 – 5,726)/14,176 = 59.61% (6,642 – 5,726)/6,642 = 13.79%			
Re	10	17.78	31.62	56.23	100	177.8	316.2	562.3	1,000

Table 12. Comparison with total iteration number for all 16 points (second example)

	Method A		Method B			Method C		
Total	27,243		13,017 (27,243 – 13,017)/27,243 = 52.22%			7,621 (27,243 – 7,621)/27,243 = 72.03% (13,017 – 7,621)/13,017 = 41.45%		
Re	10	17.78	30	31.62	50	56.23	80	100
Re	120	177.8	300	316.2	500	562.3	800	1,000

The Reynolds number is defined as

$$Re = \frac{u_{mean}H_1}{\nu} \tag{12}$$

where u_{mean} is the mean velocity at the inlet section. Reynolds number ranges from 10 to 500, and a grid system of 122×62 is adopted. In the domain $0 < X < L_1/H_1$, $0 < Y < 1$, the domain extension method [20] is used to deal with the solid region. At the outflow boundary, fully developed condition is assumed.

The saving in the total iteration times for the 8- and 15-points situations are listed in Tables 13 and 14. The comparison shows that for this problem Method C may save 47.3% to 65.8% of total iteration numbers over Method A. Once again, the example shows the efficiency of the interpolative initial fields.

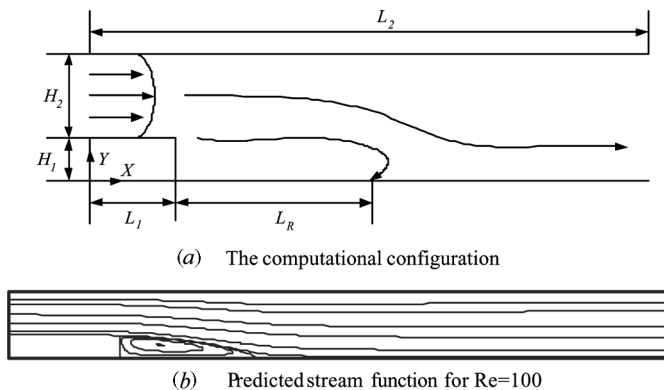


Figure 5. Laminar fluid flow over a rectangular backward step.

Table 13. Comparison with total iteration number for 8 points (third example)

	Method A		Method B			Method C		
Total	6,046		3,488 (6,046 – 3,488)/6,046 = 42.31%			3,185 (6,046 – 3,185)/6,046 = 47.32% (3,488 – 3,185)/3,488 = 8.69%		
Re	10	17.8	31.6	56.2	100	177.8	316.2	500

The following should be noted when an algorithm of the SIMPLE family is used to deal with the coupling between velocity and pressure. In our computation the left-side solid region is taken as a special fluid with very large viscosity. And the west–south corner point is taken as the reference point for the pressure. The reference pressure value should be the same for different point computation in order to make the interpolative initial pressure field meaningful.

Problem 4: Laminar Fluid Flow over an Annular Backward Step

In Figure 6, the problem configuration and its converged stream function are shown, where $L_x/D_{in} = 30$, $L_{in}/D_{in} = 5$, and $D_{out}/D_{in} = 2$.

The inlet velocity distribution is assumed to be fully developed:

$$u = u_{\max} \left(1 - \frac{r^2}{R_{in}^2} \right) \quad R_{in} = \frac{D_{in}}{2} \quad u_{\max} = 2u_{\text{mean}} \quad (13)$$

The Reynolds number is defined as

$$\text{Re} = \frac{u_{\text{mean}} D_{in}}{\nu}$$

where u_{mean} is the mean velocity at the inlet section. In the present study, Reynolds number ranges from 10 to 500, and a grid system of 202×42 is adopted. The domain extension method is used: the inlet step region of the solid is treated as a special fluid with very large viscosity [20]. At the outflow boundary, fully developed condition is assumed.

Experimental and numerical studies of this problem were carried out by Macagno and Hung [27]. They provided the following results: the ratios of the reattachment length over inlet diameter, L_R/D_{in} , as 2.2, 4.3, 6.5, and 8.8 for Re numbers

Table 14. Comparison with total iteration number for all 15 points (third example)

	Method A		Method B			Method C		
Total	10,953		5,109 (10,953 – 5,109)/10,953 = 53.36%			3,749 (10,953 – 3,749)/10,953 = 65.77% (5,109 – 3,749)/5,109 = 26.62%		
Re	10	17.8	20	31.6	50	56.2	80	100
Re	150	178	200	300	316	400	500	

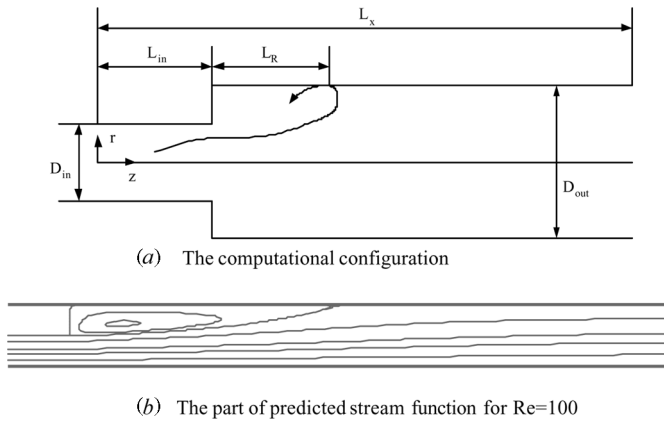


Figure 6. Laminar fluid flow over an annular backward step.

50, 100, 150, and 200, respectively. Our predicted L_R/D_{in} from the three kinds of methods are the same: 2.19, 4.40, 6.63, and 8.86 for Re number = 50, 100, 150, and 200.

The total iteration number comparisons for three situations are presented in Tables 15–17. As can be seen there, the saving in total iteration number is significant for 11 and 17 points: the total iteration number of Method C can save 40.7% and 61.7%, respectively, compared with Method A.

Problem 5: Natural Convection in a Square Cavity

As shown in Figure 7a, the square cavity has two adiabatic walls (top and bottom), with its two vertical walls being maintained at constant but different temperatures. The predicted results stream function for $Ra = 10^5$ is shown in Figure 7b, and it coincides well with that of Barakos and Mitsoulis [24].

Computations are performed for a series of simulation with Ra from 10^2 to 10^6 based on the Boussineq assumption. The Rayleigh number is defined by

$$Ra = \frac{\rho g \beta L^3 \Delta T}{\alpha \mu} \tag{14}$$

A uniform grid system of 102×102 is adopted.

Table 15. Comparison with total iteration number for 5 points (fourth example)

	Method A	Method B	Method C
Total	3,978	3,083 (3,978 – 3,083)/3,978 = 22.50%	2,709 (3,978 – 2,709)/3,978 = 31.90% (3,083 – 2,709)/3,083 = 12.13%
Re	20	50	100
			150
			200

Table 16. Comparison with total iteration number for 11 points (fourth example)

	Method A			Method B			Method C				
Total	7,337			5,360			4,350				
				$(7,337 - 5,360)/7,337 = 26.95\%$			$(7,337 - 4,350)/7,337 = 40.71\%$				
							$(5,360 - 4,350)/5,360 = 18.84\%$				
Re	1	1.778	3.162	5.623	10	17.78	31.62	56.23	100	177.8	316.2

Table 17. Comparison with total iteration number for all 17 points (fourth example)

	Method A			Method B			Method C		
Total	11,855			7,382			4,545		
				$(11,855 - 7,382)/11,855 = 37.73\%$			$(11,855 - 4,545)/11,855 = 61.66\%$		
							$(7,382 - 4,545)/7,382 = 38.43\%$		
Re	1	1.778	3.162	5	5.623	10	17.78	20	31.62
Re	50	56.23	100	150	177.8	200	300	316.2	

The cavity average Nusselt numbers for $Ra = 10^3, 10^4, 10^5,$ and 10^6 obtained in [24] are 1.114, 2.245, 4.510, and 8.806, respectively; and our predicted corresponding results are 1.13, 2.25, 4.53, and 8.91, showing very good agreement.

In Tables 18–20 the iterations number comparisons for three situations with 5, 9, and 17 points are provided. The saving with Method C compared with Method A ranges from 42.02% to 77.0%.

Problem 6: Natural Convection in an Annulus Enclosure

This test problem is for laminar natural convection between two horizontal concentric cylinders, depicted in Figure 8a. Our predicted results of stream function in Figure 8b for $Ra = 10^5$ is in good agreement with Kuehn and Goldstein’s result [28].

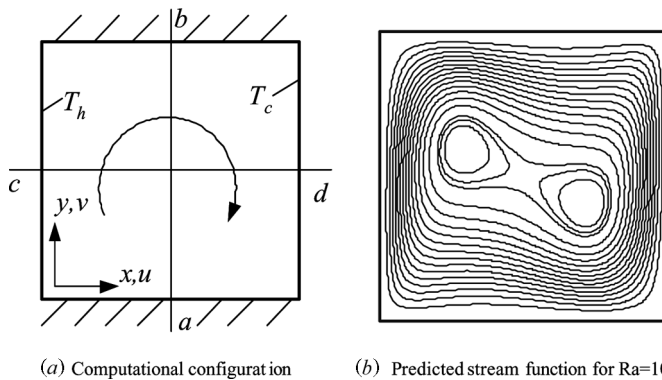


Figure 7. Natural convection in a square cavity for $Ra = 10^5$.

Table 18. Comparison with total iteration number for 5 points (fifth example)

	Method A		Method B		Method C	
Total	12,071		7,976 (12,071 – 7,976)/12,071 = 33.97%		6,998 (12,071 – 6,998)/12,071 = 42.02% (7,976 – 6,998)/7,976 = 12.25%	
Ra	100	1,000	10,000	100,000	1,000,000	

Computations are performed from $Ra = 10^2$ to 10^6 . The Rayleigh number is defined by

$$Ra = \frac{\rho g \beta \delta^3 \Delta T}{\alpha \mu} \quad (15)$$

The Boussinesq assumption is adopted. Computations are conducted on a uniform grid system with 82×62 mesh.

The comparison results shown in Tables 21–23 once again demonstrate the great advantage of the interpolative initial fields method. For the three situations with 5, 9, and 16 points, the total iteration number savings with Method C are 22.6%, 46.2%, and 65.3%, respectively, compared with Method A.

Problem 7: Three-Dimensional Slit Fin Surface Simulation

Of course, it is very disappointing if a new method is efficient only for simple problems. Thus, the advantage of Method C should be tested by a complicated 3-D

Table 19. Comparison with total iteration number for 9 points (fifth example)

	Method A			Method B			Method C		
Total	22,384			10,665 (22,384 – 10,665)/22,384 = 52.35%			8,512 (22,384 – 8,512)/22,384 = 61.97% (10,665 – 8,512)/10,665 = 20.19%		
Ra	100	316.2	1,000	3,162	10,000	31,620	100,000	316,200	1,000,000

Table 20. Comparison with total iteration number for all 17 points (fifth example)

	Method A				Method B				Method C			
Total	42,335				15,892 (42,335 – 15,892)/42,335 = 62.46%				9,738 (42,335 – 9,738)/42,335 = 77.0% (15,892 – 9,738)/15,892 = 38.72%			
Ra	100	177.8	316.2	562.3	1,000	1,778	3,162	5,623	10,000			
Ra	17,780	31,620	56,230	100,000	177,800	316,200	562,300	1,000,000				

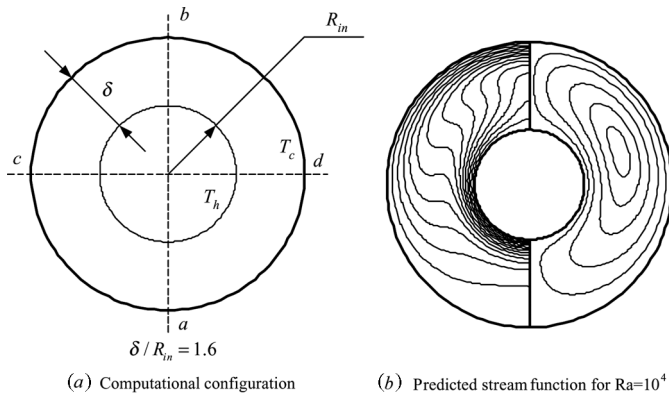


Figure 8. Natural convection in an annulus enclosure for $Ra = 10^4$.

problem. The problem of air flow and heat transfer characteristics in a three-dimensional slit fin surface is selected for this purpose.

Figure 9 shows the detail fin configurations of the slit fin. Eight straight strips with 2.5-mm width and 1.0-mm depths are just punched based on the above fin surface with 2-row tubes. The other details of the geometry can be found in [29].

The computational domain is shown in Figure 10. As can be seen there, two additional regions are added for numerical treatment purposes. The lengths of these two additional regions are 1.5 times and 5 times the streamwise fin length, respectively. This should guarantee that air velocity is uniform in the domain inlet and fully development condition obtains in the domain outlet.

The computational domain is meshed by a nonuniform $208 \times 64 \times 24$ grid system. The domain extended method is adopted to deal with the circular boundary [20], and the tube is approximated by a stepwise method.

The maximum relative mass residual of control volume and the relative difference between two successive iterates are adopted for the judging of iteration convergence:

$$\left| \frac{R_{\max}}{q_m} \right| \leq 10^{-6} \tag{16}$$

$$\left| \frac{Q_{\text{total}}^{(k+100)} - Q_{\text{total}}^{(k)}}{Q_{\text{total}}^{(k+100)}} \right| \leq 10^{-6} \tag{17}$$

Table 21. Comparison with total iteration number for 5 points (sixth example)

	Method A	Method B	Method C
Total	6,311	5,404 (6,311 - 5,404)/6,311 = 14.37%	4,884 (6,311 - 4,884)/6,311 = 22.61% (5,404 - 4,884)/5,404 = 9.62%
Ra	1,000	3,162	10,000
			31,620
			100,000

Table 22. Comparison with total iteration number for 9 points (sixth example)

	Method A		Method B				Method C			
Total	10,572		7,181				5,684			
			$(10,572 - 7,181)/10,572 = 32.08\%$				$(10,572 - 5,684)/10,572 = 46.24\%$			
							$(7,181 - 5,684)/7,181 = 20.85\%$			
Ra	1,000	1,778	3,162	5,623	10,000	17,783	31,623	56,234	100,000	

Table 23. Comparison with total iteration number for all 16 points (sixth example)

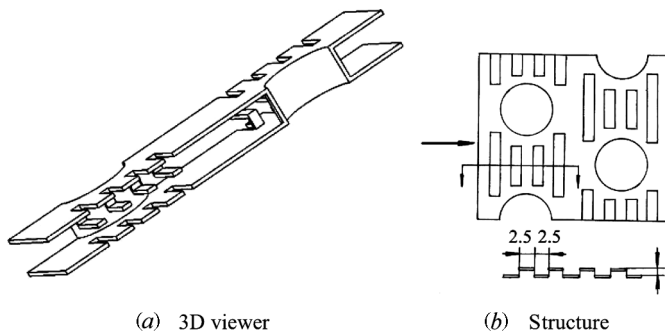
	Method A		Method B				Method C			
Total	18,090		10,413				6,285			
			$(18,090 - 10,413)/18,090 = 42.44\%$				$(18,090 - 6,285)/18,090 = 65.26\%$			
							$(10,413 - 6,285)/10,413 = 39.64\%$			
Ra	1,000	1,778	3,162	5,000	5,623	7,500	8,500	10,000		
Ra	17,783	30,000	31,623	50,000	56,234	60,000	80,000	100,000		

To show the wide applicability, for this case we choose the air velocity as the interpolative independent variable, and velocity, pressure, and temperature distributions as the interpolated functions.

Two series computations are conducted for comparison; for one series the inlet velocity varies from 0.5 to 2.5 m/s and 9 points with a 0.25-m/s interval; and for the other the inlet velocity changes from 0.5 to 3.5 m/s and 7 points with 0.5-m/s interval are used.

In Table 24 the savings in the iteration numbers for series A are listed. The ratios of total saving in CPU time for Method C over Methods A and B are up to 67.67% and 42.33%, respectively. The result is quite exciting.

In Table 25, the comparison results for the second series are provided. The ratios of total saving CPU time for Method C over Method A and B are up to 58.82%, 39.37%, respectively.

**Figure 9.** Slit fin with parallel strips.

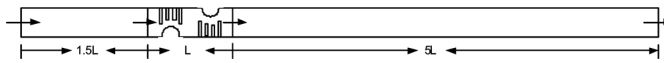


Figure 10. Top view of the computational domain.

In addition, in Table 26, a specific point, $v = 1.6$ m/s, is computed for the first series with these three kinds of methods. Based on the existing points of the first series, Method C has perfect behavior. A reduction of computational time up to one order of magnitude is obtained.

From this example, it can be found that the interpolative initial fields method is a good approach for simulation of a complicated 3-D problem.

DISCUSSION

Through the above seven examples, it is demonstrated that the interpolative initial fields method can greatly improve the convergence rate of the iterative process for a series of numerical simulations compared with the conventional methods (Method A or Method B). For these problems, generally speaking, the total saving of iteration numbers is about 23% to 77% compared to Method A, and about 3.07% to 43.39% compared to Method B. The more points are used, the more time saving can be obtained.

Obviously, for the first several points, Method C has a little advantage. Especially for the second point (always the end point), the iteration number of most problems is higher than with Method B. For Method C, it is the end point that cost the most iteration time, and it decreased the saving ratio of total iteration number. In contrast, the increase in the iteration number of later-added points can most effectively exhibit the advantage of Method C. For a series of computations, the interpolative initial fields method is very useful.

During the numerical experiment, we found that the order of computational points is also very important. According to our experience, dichotomy is the best choice. For example, if the first and second points are $Re = 10$ and $1,000$, the third point should be $Re = 100$, because it is the average logarithm value of previous two points.

Certainly, interpolation initial fields also need time for computing. Nevertheless, for any complicated problems, it is negligible. For example, for interpolation for a 3-D slit fin surface, it took less than 60 s, far less than the simulation time, which was more than several hours.

Table 24. Comparison with total CPU time

	Method A		Method B			Method C			
Total	587,173		329,137			189,827			
			$(587,173 - 329,137)/587,173 = 43.96\%$			$(587,173 - 189,827)/587,173 = 67.67\%$			
						$(329,137 - 189,827)/329,137 = 42.33\%$			
Velocity (m/s)	0.5	0.75	1.0	1.25	1.5	1.75	2.0	2.25	2.5

Table 25. Comparison with total CPU time

	Method A		Method B			Method C		
Total	456,214		309,898			187,884		
			$(456,214 - 309,898)/456,214 = 32.07\%$			$(456,214 - 187,884)/456,214 = 58.82\%$		
						$(309,898 - 187,884)/309,898 = 39.37\%$		
Velocity (m/s)	0.5	1.0	1.5	2.0	2.5	3.0	3.5	

Table 26. Comparison for $V = 1.6$ with three kinds of methods

	Method A	Method B	Method C
CPU time	75,350	20,496	3,294

CONCLUSIONS

In this article, comprehensive numerical experiments have been conducted for the interpolative initial fields method. The six 2-D and one 3-D experiments tested incompressible laminar fluid flow and heat transfer problems over three orthogonal coordinates. Numerical experiments definitely demonstrate that for a series computations the interpolative method can significantly enhance the convergence rate of the iteration process compared with the step-by-step initial fields method or without preconditioned initial fields. For the six 2-D problems tested, the interpolation method can reduce the iteration number by 3–77%. For the one 3-D problem, it can reduce the CPU time up to 40%.

REFERENCES

1. C. Prakash and S. V. Patankar, Combined Free and Forced Convection in Vertical Tube with Radial Internal Fin, *ASME J. Heat Transfer*, vol. 103, pp. 566–572, 1981.
2. G. D. Raithby and G. E. Schneider, Elliptic System: Finite Difference Method II, in W. J. Minkowycz, E. M. Sparrow, R. H. Pletcher, and G. E. Schneider (eds.), *Handbook of Numerical Heat Transfer*, pp. 241–289, Wiley, New York, 1988.
3. J. P. van Doormaal and G. D. Raithby, Enhancements of the SIMPLE Method for Predicting Incompressible Fluid Flows, *Numer. Heat Transfer*, vol. 7, pp. 147–163, 1984.
4. R. I. Issa, Solution of Implicitly Discretized Fluid Flow Equation by Operator-Splitting, *J. Comput. Phys.*, vol. 62, pp. 40–65, 1985.
5. S. V. Patankar, *Numerical Heat Transfer and Fluid Flow*, Hemisphere, Washington, DC, 1980.
6. S. V. Patankar and D. B. Spalding, A Calculation Procedure for Heat, Mass and Momentum Transfer in Three Dimensional Parabolic Flows, *Int. J. Heat Mass Transfer*, vol. 15, pp. 1787–1806, 1972.
7. U. Ghie, K. N. Ghie, and C. T. Shin, High-Re Solutions for Incompressible Flow Using the Navier Stokes Equations and a Multigrid Method, *J. Comput. Phys.*, vol. 48, pp. 387–411, 1982.
8. W. Q. Tao, Z. G. Qu, and Y. L. He, A Novel Segregated Algorithm for Incompressible Fluid Flow and Heat Transfer Problems—CLEAR (Coupled and Linked Equations

- Algorithm Revised) Part II: Application Examples, *Numer. Heat Transfer B*, vol. 45, pp. 19–48, 2004.
9. W. Q. Tao, Z. G. Qu, and Y. L. He, A Novel Segregated Algorithm for Incompressible Fluid Flow and Heat Transfer Problems—CLEAR (Coupled and Linked Equations Algorithm Revised) Part I: Mathematical Formulation and Solution Procedure, *Numerical Heat Transfer B*, vol. 45, pp. 1–17, 2004.
 10. S. V. Patankar, A Calculation Procedure for Two-Dimensional Elliptic Situations, *Numer. Heat Transfer*, vol. 4, pp. 409–425, 1981.
 11. W. Q. Tao, *Recent Advances in Computational Heat Transfer*, Science Press, Beijing, 2000.
 12. S. Sebben and B. R. Baliga, Some Extensions of Tridiagonal and Pentadiagonal Matrix Algorithms, *Numer. Heat Transfer B*, vol. 28, pp. 323–357, 1995.
 13. C. J. Kim and S. T. Ro, A Block-Correction Aided Strongly Implicit Solver for the Five-Point Formulation of Elliptic Differential Equations, *Int. J. Heat Mass Transfer*, vol. 208, pp. 999–1008, 1995.
 14. A. Jennings and J. J. McKeown, *Matrix Computation*, Wiley, Chichester, UK, 1992.
 15. W. J. Minkowycz, E. M. Sparrow, G. E. Schneider, and R. H. Pletcher, *Handbook of Numerical Heat Transfer*, Wiley, New York, 1988.
 16. W. F. Ames, *Numerical Methods for Partial Differential Equations*, Academic Press, New York, 1977.
 17. H. L. Stone, Iterative Solution of Implicit Approximations of Multidimensional Partial Differential Equations, *SIAM J. Numer. Anal.*, vol. 5, no. 3, pp. 530–558, 1968.
 18. M. R. Hestens and E. Stiefel, Methods of Conjugate Gradients for Solving Linear Systems, *J. Res. Natl. Bur. Std.*, vol. 49, pp. 409–436, 1952.
 19. F. Moukalled and M. Darwish, A Unified Formulation of the Segregated Class of Algorithm for Fluid Flow at All Speeds, *Numer. Heat Transfer B*, vol. 37, pp. 103–139, 2000.
 20. W. Q. Tao, *Numerical Heat Transfer*, 2d ed., Xi'an Jiaotong University Press, Xi'an, China, 2001.
 21. P. H. Gaskell, A. K. C. Lau, and N. G. Wright, Comparison of Two Solution Strategies for Use with Higher-Order Discretization Schemes in Fluid Flow Simulation, *Int. J. Numer. Meth. Fluids*, vol. 8, pp. 1203–1215, 1988.
 22. H. W. Lin and L. D. Chen, Application of Krylov Subspace Method to Numerical Heat Transfer, *Numer. Heat Transfer A*, vol. 30, pp. 249–270, 1996.
 23. T. Kondoh, Y. Nagano, and T. Tsaji, Computational Study of Laminar Heat Transfer Downstream of a Backward Facing Step, *Int. J. Heat Mass Transfer*, vol. 36, no. 3, pp. 577–591, 1993.
 24. G. Barakos and E. Mitsoulis, Natural Convection Flow in a Square Cavity Revisited: Laminar and Turbulent Methods with Wall Functions, *Int. J. Numer. Meth. Fluids*, vol. 18, no. 7, pp. 695–719, 1994.
 25. R. L. Burden and J. D. Faires, *Numerical Analysis*, 7th ed., Brooks/Cole, 2001.
 26. L. Fuchs and N. Tillmark, Numerical and Experimental Study of Driven Flow in a Polar Cavity, *Int. J. Numer. Meth. Fluids*, vol. 5, pp. 311–329, 1985.
 27. E. O. Macagno and T. K. Hung, Computation and Experimental Study of Captive Annular Eddy, *J. Fluid Mech.*, vol. 28, pp. 43–64, 1967.
 28. T. H. Kuehn and R. J. Goldstein, An Experimental and Theoretical Study of Nature Convection in the Annulus between Horizontal Concentric Cylinders, *J. Fluid Mech.*, vol. 74, pp. 695–715, 1969.
 29. R. C. Xin, H. Z. Li, H. J. Kang, et al., Experimental Study on Heat Transfer and Pressure Drop Characteristics of Four Types of Plate Fin-and-Tube Heat Exchanger Surface, in *Transport Phenomena Science and Technology*, pp. 942–947, Higher Education Press, Beijing, China, 1992.